

## **DETERMINISTIC RADIATION TRANSPORT SIMULATIONS FOR DIAGNOSTIC IMAGING APPLICATIONS**

**Monica Ghita, Glenn E. Sjoden**

Department of Nuclear and Radiological Engineering  
University of Florida, 202 NSB, Gainesville, FL, 32611  
[ghita1mc@ufl.edu](mailto:ghita1mc@ufl.edu); [sjoden@ufl.edu](mailto:sjoden@ufl.edu)

**Ahmad Al-Basheer**

Georgia Radiation Therapy Center  
Medical College of Georgia, Augusta, GA 30912  
[aalbasheer@mail.mcg.edu](mailto:aalbasheer@mail.mcg.edu)

**Manuel M. Arreola**

Department of Radiology  
University of Florida  
PO Box 100374, Gainesville, FL 32610-0374  
[arreom@radiology.ufl.edu](mailto:arreom@radiology.ufl.edu)

**Wesley Bolch, Choonsik Lee**

Department of Nuclear and Radiological Engineering/ALRADS Group  
University of Florida, 202 NSB, Gainesville, FL, 32611  
[wbolch@ufl.edu](mailto:wbolch@ufl.edu); [leecs@ufl.edu](mailto:leecs@ufl.edu);

### **ABSTRACT**

Monte Carlo methods have been established along the time as the gold standard for computer simulations in the medical physics community. Depending on the problem and user's needs, deterministic radiation transport simulations may provide a more detailed and faster solution. In this work we investigate the possibility of using deterministic radiation transport simulations as a viable and more convenient tool for real clinical applications. Therefore, the discrete ordinates PENTRAN code is used to calculate average organ doses in voxelized human phantoms and the results are compared with state-of-the-art MCNP5 Monte Carlo simulations in the diagnostic energy range (50-140 keV). Generally, good agreement for the average organ scalar fluxes, less than 6% difference, is obtained provided adequate quadrature order, mesh size and energy group structure is used in the deterministic calculations. The energy group structure, particularly for the diagnostic energy range, has a major impact on the deterministic solution for the average organ doses since the interaction and mass energy absorption coefficients are highly energy dependent in the diagnostic range. Though an optimization of the group structure is possible, it is problem (namely x-ray source spectrum) and organ dependent, which impose serious limitations of the deterministic solution for practical application in diagnostic medical physics.

*Key Words:* Radiation transport, deterministic discrete ordinates, Monte Carlo, voxelized phantom, average organ dose

## 1. INTRODUCTION

Modern radiation dosimetry methods depend increasingly on human anatomical modeling and radiation transport simulation. Regardless of the means by which an ionizing radiation dose is delivered, neutral particle transport and interactions of the radiation can be precisely determined via solution of the linear Boltzmann or “transport” equation (Eq. 1), which describes the behavior of neutral particles as a function of the spatial, angular, and energy domains.

$$\hat{\Omega} \cdot \nabla \psi(\vec{r}, \hat{\Omega}, E) + \sigma(\vec{r}, E) \psi(\vec{r}, \hat{\Omega}, E) = \int_0^{\infty} \int_{4\pi} dE' d\Omega' \sigma_s(\vec{r}, \hat{\Omega}' \cdot \hat{\Omega}, E' \rightarrow E) \psi(\vec{r}, \hat{\Omega}', E') + Q(\vec{r}, \hat{\Omega}, E) \quad (1)$$

The left side of Eq. 1 represents streaming and collision terms (loss), and the right side represents scattering and other sources (gain),  $\psi$  being the angular flux of particles in the phase space as a function of position, energy, and direction, and  $Q$  the density of source particles emitted in the same phase space. The Boltzmann equation can be precisely solved by following two main approaches, both based on first principles: statistical Monte Carlo and deterministic solution methods.

In the statistical Monte Carlo approach, one solves for the expected value of particle density in the phase space by averaging over a large number of particle histories or events. An alternative to Monte-Carlo-based radiation dose calculations can be achieved by a deterministic solution of the Boltzmann equation that models radiation transport through materials. A common approach for calculating radiation doses using the Boltzmann equation is known as the “discrete-ordinates” method. This approach discretizes the radiation-transport equation in space (finite-difference or finite-element), angle (discrete-ordinates), and energy (via multi-group cross sections), and then iteratively solves the integro-differential form of the transport equation over a discrete, multi-dimensional space. Both approaches are very powerful, and can lead to accurate solutions; however, depending on the problem type and overall objective, one approach can be more effective than the other, depending upon the problem being solved.

The dramatic evolution of imaging over the past quarter century has also resulted in a significant increase in the population’s cumulative exposure to ionizing radiation. There is therefore a serious demand for more accurate and reasonably fast, patient specific dose evaluation methods for diagnostic imaging. To serve this goal, we developed PENTRAN-MP, a specialized code package for medical physics applications based on deterministic radiation transport simulations. In this work we compare the average doses for the most radiosensitive organs calculated using our developed deterministic code system with the state-of-the-art (quasi-continuous source spectrum, continuous ENDF/B-VI cross-section library) MCNP5 [1] Monte Carlo simulations. Both set of simulations are done employing the 11 year male phantom from the UF Series B voxelized pediatric phantoms [2].

## 2. MATERIALS AND METHODS

Monte Carlo methods have evolved over time as the ‘gold standard’ for computer simulations in the medical physics community. Depending on the problem and user’s needs, deterministic radiation transport simulations may provide a more detailed, faster solution, since it yields a global phase space solution. The accuracy and efficiency of the deterministic methods have been

well demonstrated for nuclear reactor and detection problems, but have yet to be proven for wide use in medical physics applications. To investigate the possibility of using deterministic radiation transport simulations as a viable tool in real clinical applications, we developed a code system, PENTRAN-MP, and a methodology (Fig. 1) for patient radiation dose calculations using voxelized human phantoms.

PENTRAN-MP is a package of existing (PENTRAN[3,4], PENMSHXP[3], PENDATA[3], CEPXS[5]) or specially developed (DXS[6], GREPXS, GHOST-3D, 3D-DOSE) codes to facilitate the simulation methodology, which is organized in three stages of calculation: pre-processing (GHOST-3D, DXS, PENMSHXP and CEPXS), radiation transport calculation (PENTRAN), and post-processing (PENDATA and 3D-DOSE).

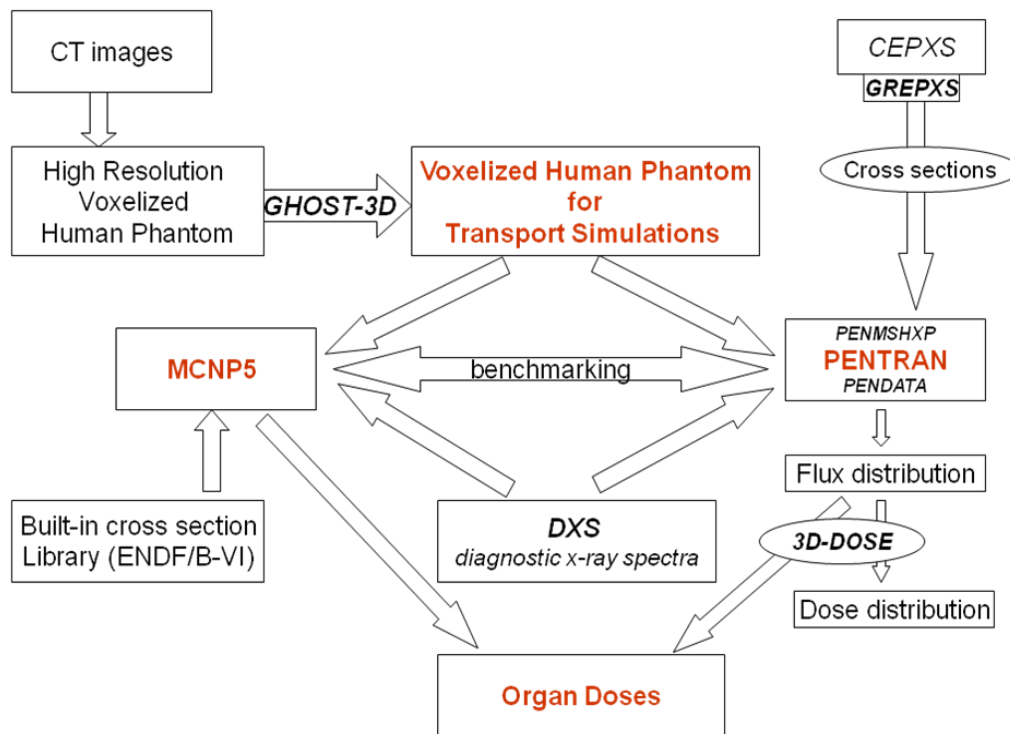


**Figure 1. Simulation methodology for dose distribution and organ dose calculations using the PENTRAN-MP code system**

## 2.1. PRE-PROCESSING CODES

### 2.1.1 PENMSHXP – PENTRAN’s input file generator

PENMSHXP, the code developed by Yi and Haghghat, is a 3-D Cartesian-based mesh generator that prepares material and source distributions for the PENTRAN particle transport code. As part of the PENTRAN-MP package, PENMSHXP has been adapted to read two binary input files,

one for the phantom geometry containing the material distribution (which can be established from actual CT data), and another one with the radiation activity value for each voxel/fine mesh (which can be used to specify the fixed source distribution in the model) and to combine them to generate the input deck for the PENTRAN transport calculations.

### **2.1.2 DXS – the pilot code of the PENTRAN-MP system**

Usually, a deterministic transport simulation may require a considerable amount of time and effort to prepare all the necessary ingredients for the actual execution. Also, there may be considerable effort involved in the post-processing of the large amount of data generated. To ease and streamline this effort, which is of great importance in a commonly busy clinical environment, the DXS code, which generates x-ray spectra in the diagnostic radiographic range [6], has been designated as the pilot code in the PENTRAN-MP system and dose computation methodology. Several options have been implemented in the code that make DXS an important tool to conveniently and consistently prepare input or part of the input files, as well as intermediate files needed for the proper execution of other codes in all the stages of a simulation. Namely, it generates the file containing the energy group probabilities in the right order (high to low energies) and format to be used by PENMSHXP to write the source definition section of the PENTRAN input deck. It also prepares a complete input file (“cepin”) for CEPXS, the multigroup macroscopic cross sections mixer, a product of Sandia National Laboratories [5]. This capability is extremely convenient, considering the large number of materials (each with several components of different content) that makes up the voxelized phantoms, as well as the non-standard way in which the parameters required for cross section calculations are defined in CEPXS. It must be mentioned that the CEPXS original code had to be debugged and modified to accommodate the large number of materials, elemental components per material, and energy groups involved in the specific simulations needed for this work. DXS also writes the “sdef” card with the energy bin bounds (“SI”-source information) and bin probabilities (“SP”-source probability) for a corresponding MCNP5 simulation. In support of the post-processing stage, DXS provides the mid-energies of the energy groups employed in the radiation transport simulation needed by 3D-DOSE to convert the calculated flux into dose.

### **2.1.3 GREPXS – the cross sections extractor and writer**

GREPXS is a small but very useful code designed to strip from the CEPXS output file the problem’s specific cross sections, and write them in a proper format that can be automatically read by PENTRAN during the execution of the transport simulation.

### **2.1.4 GHOST-3D – computational human phantoms builder**

A key factor to guarantee accurate results with our dose computation methodology is the availability of exact anatomical models for the human body. The ALRADS group at UF has built a state-of-the-art series of high resolution voxelized human phantoms using CT images of live patients [2]. These phantoms are very large arrays of numbers assigned to the different anatomical tissues and organs; for example, the matrix size for the 11 year old male phantom used in this work is 398 x 242 x 252, which directly translates in more than 24 million meshes in the computational model. Due to several constraints in simulating such big models, like limited computer memory, large running time, slow convergence, or unphysical oscillations in the

solution, GHOST-3D code has been developed to provide an equivalent model with a down-sampled number of total meshes (adjustable, depending on the user requirements), overcoming the mentioned difficulties. GHOST-3D transforms the high resolution phantom into a coarser one by “down sampling” adjacent voxels (of variable number, user dependent, on each Cartesian direction) and assigning to the equivalent voxel the dominant and closest approaching material tag number with an averaged density. As a result of this transformation, the geometrical volume and the mass of the phantom are conserved, but the size and shape of internal organs are shifted by varying degrees, depending upon the “collapsing” steps applied (Fig.2). Inevitably, a significant price may be paid in certain situations for this computational gain: some tiny organs may vanish during the “down sampling” procedure.

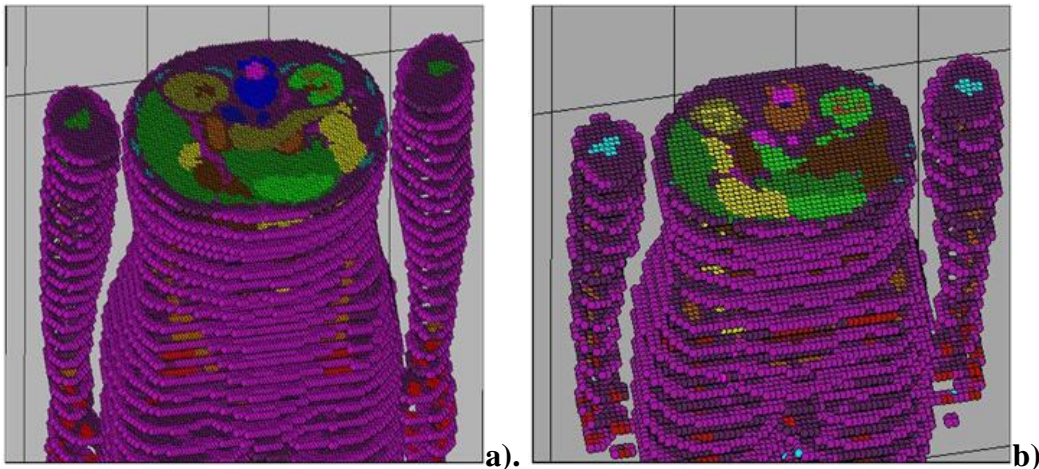


**Figure 2. GHOST-3D down-sampled models of the 11 year old male phantom of UF Series B (398 x 242 x 252 voxels, 73 materials); a). 3 x 3 x 3 collapsing steps, resulting in a 132 x 80 x 84 voxels model (72 materials), b). 5 x 5 x 5 collapsing steps, resulting in a 79 x 50 x 48 voxels model (66 materials)**

The GHOST-3D generated material distribution is written in a binary file, which is processed by PENMSHXP to generate a PENTRAN computational model and also in a text file, with the correct format, so that it can be directly included in the MCNP5 input deck. GHOST-3D writes also the file with all the information needed by PENMSHXP to provide the complete input deck for the PENTRAN radiation transport simulation. An auxiliary file, containing the tag number for each fine mesh of the deterministic model in the indexing order defined in PENTRAN, is also produced to be used in the post-processing stage for converting the scalar flux into dose.

## 2.2. PENTRAN - A DETERMINISTIC DISCRETE ( $S_N$ ) CODE

PENTRAN (Parallel Environment Neutral-particle TRANsport) is a multi-group, anisotropic  $S_N$  code that solves the time-independent linear Boltzmann equation using finite-volume differencing in 3D- Cartesian geometries; it has been specifically designed for distributed memory, scalable parallel computer architectures using the MPI (Message Passing Interface) library [4]. Automatic domain decomposition among the angular, energy, and spatial variables

with an adaptive differencing algorithm and other numerical enhancements make PENTRAN an extremely robust solver. Numerous simulations have been performed using the PENTRAN code system, including many international benchmark computations.

### 2.3. POST-PROCESSING

Post processing in the PENTRAN-MP code system includes seamless parallel data extraction using the PENDATA code developed by Sjoden and Haghghat to generate the group dependent scalar flux distribution,  $\phi_{g,i}$ , in the phantom which is converted into a dose distribution. This is performed by 3D-DOSE, which applies Eq. 2 to compute the dose in each voxel,  $D_i$ , using fitting functions for the mass-energy absorption coefficients,  $(\mu/\rho)_{en,g}$ , of four materials (dry air, ICRU-44 lung tissue, ICRU-44 soft tissue and ICRU-44 cortical bone), where  $G$  is the number of energy groups used, and  $E_g$  the group midpoint energy.

$$D_i = \sum_{g=1}^G E_g \left( \frac{\mu}{\rho} \right)_{en,g} \phi_{g,i} \quad (2)$$

The values of the mass energy-absorption coefficients, as a function of photon energy, for these compounds were obtained from the NIST database. The code reports a spatial dose distribution for each energy group, total dose distribution, doses for user-selected organs, and, optionally, dose volume histograms.

### 2.4. MCNP5 – AN OPEN-SOURCE GENERAL-PURPOSE MONTE CARLO CODE

The widespread acceptance of computational models in radiation dosimetry was made possible by the availability of well-validated and maintained Monte Carlo codes. Among them, MCNP5, developed by the Los Alamos National Laboratory, is a Monte Carlo N-Particle code that can be used for neutron, photon, electron, or coupled neutron/photon/electron transport [1]. The code treats an arbitrary three-dimensional configuration of materials in geometric cells, having a generalized input capability that allows a user to model a variety of source and detector conditions. The “lattice structure” feature facilitates the definition of repeated “cells”. Pointwise cross-section data typically are used, although group-wise data also are available.

### 2.5. UF’s SERIES B VOXEL PHANTOMS

Following the development of UF’s CT-Contours segmentation software, and the construction of the first tomographic dosimetry model (UF Newborn), a series of pediatric tomographic phantoms were constructed using live patient CT images from Shands hospital image archives [7]. While these phantoms preserved the body dimensions and organ masses as seen in the original patients who were scanned, comprehensive adjustments were made for the Series B phantoms to better match International Commission on Radiological Protection (ICRP) age-interpolated reference body masses, body heights, sitting heights and internal organ masses. The

CT images of arms and legs of a Korean adult were digitally rescaled and attached to each phantom of the UF series. After completion, the resolutions of the phantoms for the 9-month, 4-year, 8-year, 11-year and 14-year were set at  $0.86 \text{ mm} \times 0.86 \text{ mm} \times 3.0 \text{ mm}$ ,  $0.90 \text{ mm} \times 0.90 \text{ mm} \times 5.0 \text{ mm}$ ,  $1.16 \text{ mm} \times 1.16 \text{ mm} \times 6.0 \text{ mm}$ ,  $0.94 \text{ mm} \times 0.94 \text{ mm} \times 6.00 \text{ mm}$  and  $1.18 \text{ mm} \times 1.18 \text{ mm} \times 6.72 \text{ mm}$ , respectively.

### 3. RESULTS AND DISCUSSION

Preliminary tests using the 11 year male phantom of the UF Series B proved that with an adequate quadrature, mesh size, and cross-section library, it is possible to produce results with the PENTRAN discrete ordinates code that agree within the statistical uncertainty of the “on-source-axis” MCNP5 Monte Carlo calculations for the proposed model [8]. Parallel deterministic PENTRAN results were obtained within comparable running times to parallel MCNP5 Monte Carlo calculations for tally sites adjacent to the source. A major advantage of the  $S_N$  method is that it provides a detailed, accurate flux distribution at thousands of cells throughout the system, while the Monte Carlo method only provides highly accurate values for selected points near the source. However, in diagnostic imaging, of main interest are average organ doses rather than dose distributions. Hence, in the present work, the same UF Series B phantom was used to evaluate the solution accuracy and computational efficiency (computer memory requirements, execution times) of the deterministic method when compared to state-of-the-art Monte Carlo simulations for organ dose calculations.

For clarity, several items related to this set of calculations require mention:

- Deterministic radiation transport in the high resolution phantom cannot be performed on commodity parallel clusters (10's of processors) due to insufficient computer memory (in spite of scalable memory options); however, even simulations using a partial model (for example, just torso of the phantom) may be challenging due to the difficulty in converging the solution, especially for the low energy groups. This behavior is to a degree problem dependent, and is also subject to the energy structure and available capacity of the parallel machine architecture; with thousands of processors available, it is conceivable that little to no down sampling may be needed, although we have not scaled problems to this level at this time.
- Very long execution times are needed for Monte Carlo simulations in the full high resolution phantom; this is since poor statistics will result as one attempts to tally histories out of field.
- For the purpose of this particular set of tests, a “state-of-the-art” Monte Carlo simulation means radiation transport using the same down-sampled voxelized model as in the deterministic calculations, but using a quasi-continuous (0.5 keV energy bins) source energy spectrum as opposed to the multi-group binned spectrum.
- To preserve a reasonable degree of detail in the computational phantom, the high-resolution phantom was down-sampled based on the dominant material method of GHOST-3D code to (79 x 48 x 125) matrix size with 4.7 mm x 4.7 mm x 12 mm voxel size (all the organs/tissues were preserved excepting the lens of the eye).

- The x-ray radiation field was model as a thin parallelepiped,  $21 \times 0.5 \times 30 \text{ cm}^3$  in the very close proximity of the phantom's chest, isotropically irradiating the phantom

Subsequently, using PENMESH-XP, the collapsed model was cast into a 3-D spatial distribution and sub-divided into six coarse mesh z-levels, with five coarse meshes in x-y domain containing a corresponding number of fine mesh cells (Fig. 3). The GHOST-3D ASCII formatted matrix file containing the material spatial distribution in the down-sampled phantom was incorporated into a lattice defined input, with same multi-group source definition, for equivalent MCNP5 simulations.

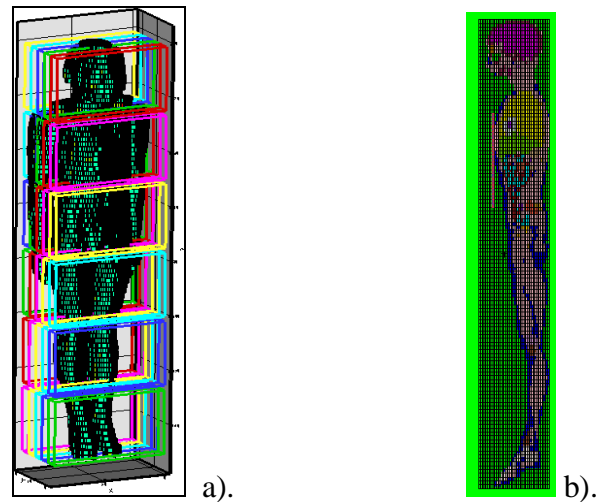


**Figure 3. PENTRAN a). and MCNP5 b). computational model**

There are several ways to compute dose using MCNP5 tallies. One can use F4 tally to compute the photon flux and then convert it to dose by multiplying with appropriate mass energy absorption coefficients using an FM card. A more convenient and direct way is to obtain the energy deposited by the photon beam in the selected region (cell) using an MCNP5 F6 tally card with the proviso that charged particle equilibrium (CPE) is valid in the tallied region. This is justified since, for the x-ray radiographic energy range, the range of secondary electrons produced is smaller than the voxel dimensions used in the model. Moreover, the atomic number of the materials present in the model is relatively low, excluding major production of bremsstrahlung radiation. So, practically all of the energy is deposited locally, and consequently kerma is equal to dose. This fact was confirmed by obtaining the same results with MCNP5 F6 and \*F8 (the latter of which scores all the photons and secondary electrons to obtain the energy deposited) tallies for even the smallest organs. Hence, all the doses in the MCNP5 simulations were obtained using an F6 tally in “mode p” code execution (which provides a significant savings in the execution time because the electrons, though accounted for, are not explicitly transported throughout the model).

To ensure that any unphysical oscillations that may result in deterministic solution are eliminated, after several tests,  $S_{48}$  Legendre-Chebyshev quadrature order [9] was chosen for the deterministic calculations.

Several energy group structures for the source spectrum and for the multi-group cross sections were tested in the attempt to optimize the deterministic transport calculations. The same 80 kVp energy spectrum (2 mm Al, 140 cm air) produced by DXS was rebinned in 8, 16, 24, and 32 energy groups, as shown in Fig.4. Fig. 5 displays the percent difference between the average organ doses calculated with PENTRAN-MP methodology and with “state-of-the-art” MCNP5 simulation.

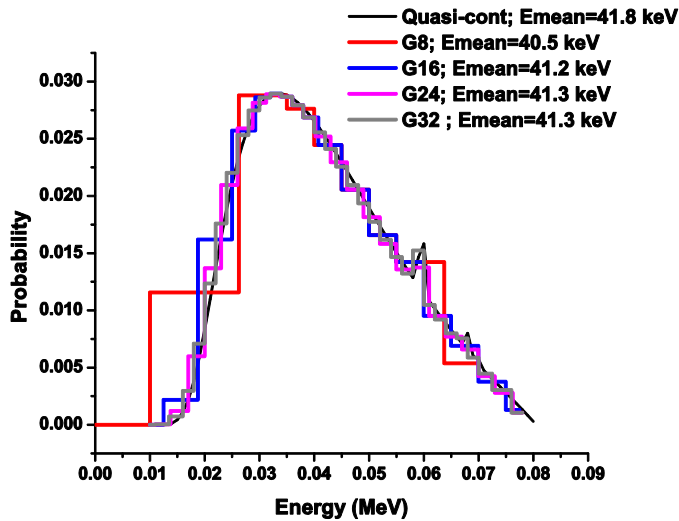


**Figure 4. Energy bin probabilities (color lines) for the  $S_{48}$  calculations generated by DXS; black line – the corresponding quasi-continuous DXS generated spectrum used in the state-of-the-art MCNP5 simulation**

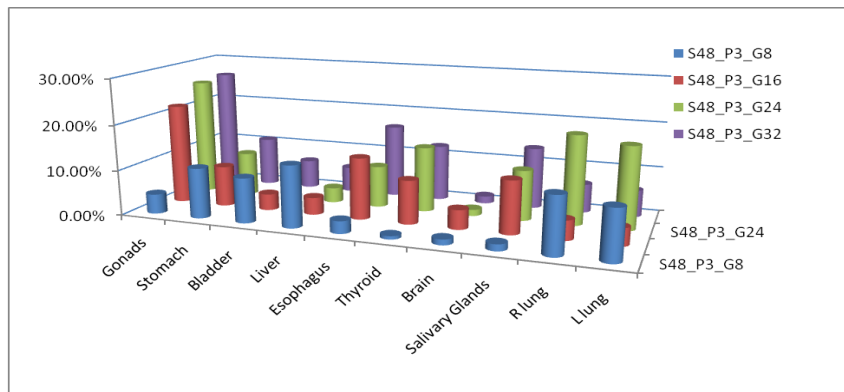


**Figure 5. Percent difference from state-of-the-art MCNP5 results of the average organ doses calculated with PENTRAN-MP methodology using different energy group structures**

Overall, the best results were obtained using 8 energy groups. In the attempt to understand this counterintuitive result, the effect of the energy group structure on the energy dependent computational components (source spectrum, cross sections, and mass energy absorption coefficients) has been studied. To estimate the effect of the bin structure of the source energy spectrum on the computed organ doses, MCNP5 calculations were performed using the same 8 group energy spectrum, and the results were compared with an  $S_{48}$  discrete ordinates computation and state-of-the-art MCNP5 ones. The percent difference for the before mentioned comparison is shown in Fig.6. Analyzing the graph, one may be tempted, generally, to correlate the differences in the calculated doses with the differences due to the source energy bin probabilities. However, as the comparison between same multi-group calculations (MCNP5 and PENTRAN) reveal, the macroscopic cross sections (flat averaged over the energy bin) and the mass absorption coefficients play an important role. This statement is supported also by the fact that MCNP5 simulations for another energy spectrum (80 kVp,  $10^\circ$  target angle, 1.2 mm Al) using the same phantom yielded very similar values for all the organ doses independent of the number of energy bins, which were linearly spaced (the spectrum was partitioned in 8, 14, and 35 energy bins and compared to the quasi-continuous spectrum). However, when a *varying* energy bin interval was considered for the 8 group simulation, 2 to 9% differences from the reference case were obtained for the calculated doses. However, when a varying energy bin interval was considered for the 8 group simulation, 2 to 9% differences from the reference case were obtained for the calculated doses. In the case of the previously discussed spectrum (80 kVp,  $12^\circ$  target angle, 2 mm Al), linearly spacing the energy range in 8 groups affected less than 1% the values of the MCNP5 calculated organ doses compared to the corresponding state-of-the-art MC simulations, while the  $S_{48}$  yielded results were 1 to 12 percent different, depending on the organ, and overall worse than the variable energy bin structure 8 group calculation.

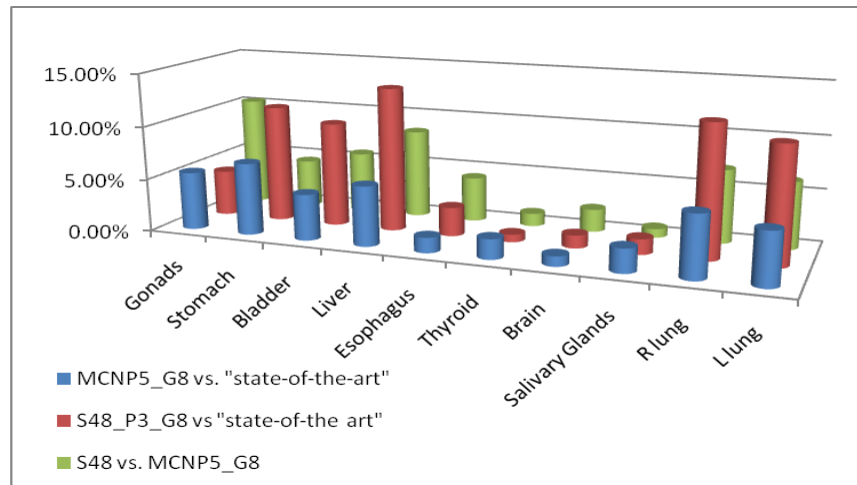


**Figure 6. Comparison between average organ doses due to the same x-ray radiation exposure, but calculated using different simulations: deterministic 8 group (S48\_P3\_G8), MCNP5 8 group energy spectrum with continuous cross sections (MCNP5\_G8), “state-of-the-art” MCNP5**

The comparison between the average organ fluxes obtained with the different deterministic calculations and the “state-of-the-art” MCNP5 simulation (Fig.7) shows a better and less energy group structure dependent agreement than the doses, but still same organ specific behavior.

This difficulty in predicting the simulation behavior is expected, considering the huge variation of the interaction and mass absorption coefficients of low Z (atomic number) materials involved in these simulations for the radiographic x-ray energy range (Fig.8). In 3D-DOSE, the scalar fluxes are converted into absorbed doses based on analytical fitting functions considering the median energy of each energy group. While the mass energy absorption coefficient is highly energy dependent over almost all the diagnostic range, the attenuation coefficient shows this dependence only for the low energy x-rays. It is therefore why the deterministic fluxes agree much better than the respective doses with the corresponding MC reference ones. Moreover, the photon (primary and scatter) spectrum is different for each individual organ and hence, this leads to the erratic effect of the energy group structure on the associated doses. We can speculate that the 8 group (variable energy bin) calculation seems to provide the best overall solution due to the broad low energy bin, where the most severe approximations for the source, cross section and absorption coefficients combined may average out better than for thinner energy bins. It can be concluded that the energy group structure considerably impacts the accuracy of the deterministic solution for the radiographic x-ray radiation transport through human phantoms. Though an optimization (depending on the level of accuracy needed) for the energy group structure is possible, it is not only problem but also individual organ dependent, which imposes substantial limitations for the deterministic method for practical diagnostic applications. Other work has shown that it is indeed quite viable for therapy photon energies (facilitated by the fact that the photon interaction coefficients for the materials of interest in these applications are significantly more slowly varying in the therapy energy range), using electron dose kernels [10].

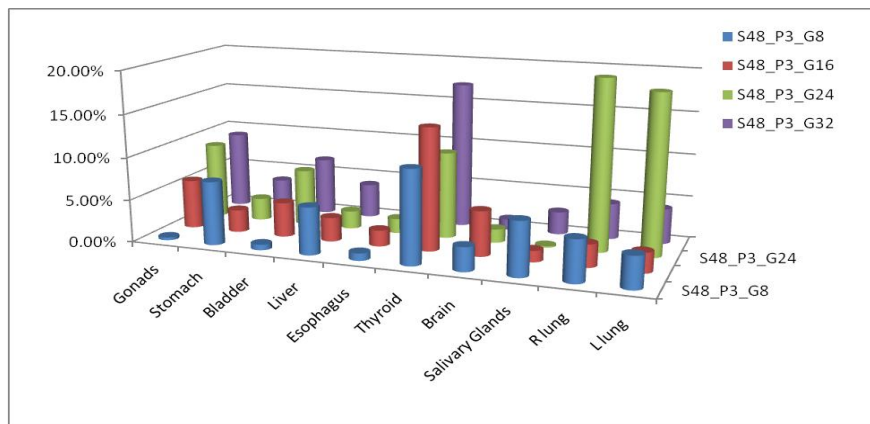


**Figure 7. Percent difference from state-of-the-art MCNP5 results of the average organ fluxes calculated with PENTRAN-MP methodology using different energy group structures**

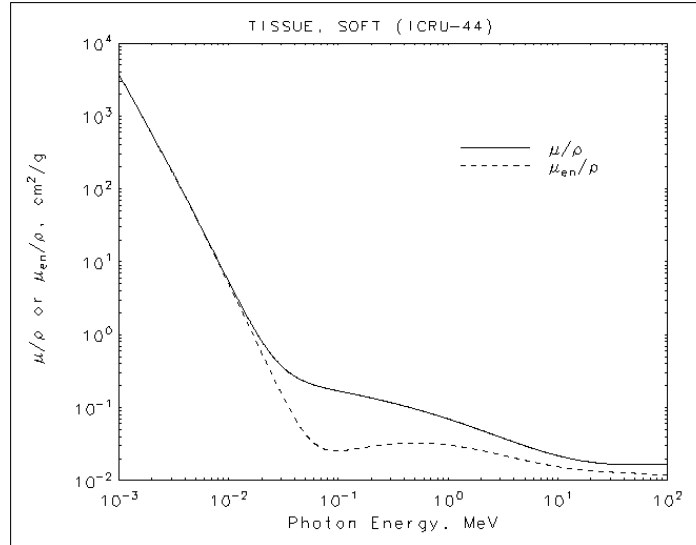


**Figure 8. Mass attenuation and mass-energy absorption coefficients for soft tissue**

### 3. CONCLUSIONS

The PENTRAN-MP code system has been developed to support the deterministic radiation transport methodology proposed for accurate and rapid dose assessments in medical physics applications. For similar multi-group calculations, PENTRAN and MCNP5 scalar flux results agree very well in the radiation field. If the global dose distribution in a complete voxelized human phantom is the objective of a calculation, then the deterministic method is preferable, since it yields a converged solution over the entire system, solution whose accuracy cannot be easily established with Monte Carlo, since stochastic simulations cannot provide whole body results (in a reasonable time) with enough precision for reliable comparison.

For patient dosimetry in diagnostic imaging modalities, of major importance are organ doses. If evaluation of organ doses using the deterministic approach assumes the same execution time as that for entire system dose distribution calculation, in the Monte Carlo simulation there is a significant reduction in the computational time (tallies are scored in bigger volumes, with better statistics in less time). Moreover, the tests demonstrated that the accuracy of the deterministic solution critically depends on the energy group structure. Due to the steep variation with energy of the interaction coefficients for the organ and tissues in the human body in the radiographic energy range (50-150 keV), it is a real challenge to optimize an energy group structure for deterministic simulations. This optimization is problem/objective dependent and needs to be performed for every source energy spectrum and almost for every organ in part. Generation of special weighted cross sections and mass energy absorption coefficients in the radiographic energy range may overcome the present difficulties. Hence, it can be concluded that, at this stage, the PENTRAN-MP methodology is a potential solution due to its numerical accuracy and sound algorithms for applications specifically calling for whole body dosimetry, but is not ready yet to be employed for challenging organ specific diagnostic dose calculations; other work has shown that it is quite viable for therapy photon energies when coupled to electron dose kernels under the recently developed EDK- $S_N$  procedure.

## REFERENCES

1. "MCNP5- A General Monte Carlo N-Particle transport code", Version 5, LA-UR-03-1987, Los Alamos National Laboratory, 2003.
2. C. Lee, C. Lee, J. L. Williams, and W. E. Bolch, "Whole-body voxel phantoms of paediatric patients--UF Series B," *Phys.Med.Biol.*, **51**, pp.4649-4661 (2006).
3. H&S ACT, Inc: PENTRAN<sup>TM</sup>, PENMSH<sup>TM</sup>, and 3DI<sup>TM</sup>, are trademarks of H&S Advance Computing Technologies, Inc, <http://www.hsact.com> (2001)
4. G. E. Sjoden. and A. Haghghat, "PENTRAN - A 3-D Cartesian Parallel Sn Code with Angular, Energy, and Spatial Decomposition," *Proceeding of Joint Int'l Conf on Mathematical Methods and Supercomputing in Nuclear Applications*, Saratoga Springs, NY, Vol. II, pp.1267-1276 (1997).
5. L. J. Lorence, J. E. Morel, et al., "Physics Guide to CEPXS: A multigroup coupled electron-photon cross section generating code," (1989).
6. M. Ghita, G. E. Sjoden, and M. M. Arreola, "Validation of DXS: a Diagnostic X-ray Spectra generator", submitted to *Med. Phys*
7. C. Lee, J. L. Williams, C. Lee, and W. E. Bolch, "The UF series of tomographic computational phantoms of pediatric patients," *Med.Phys.*, **32**, pp.3537-3548 (2005).
8. A. Al-Basheer, M. Ghita, G. E. Sjoden, W. Bolch, and C. Lee, "Whole Body Dosimetry Simulations using the PENTRAN-MP Sn Code System," *American Nuclear Society, Annual Meeting*, Boston, MA, pp.66 (2007)
9. G. Longoni and A. Haghghat, "Development of new quadrature sets with the Ordinate Splitting technique", *Proceedings of the ANS International Meeting on Mathematical Methods for Nuclear Applications*, Salt Lake City UT, (2001).
10. A. Al-Basheer, G. Sjoden, and M. Ghita, "Electron Dose Kernels to Account for Secondary Particle Transport in Deterministic Simulations", accepted, *Nuclear Technology Journal*, September, 2008, 19 pages (manuscript).